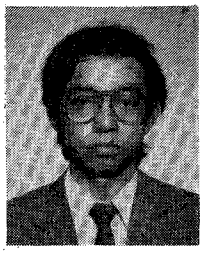

Yoshio Obata was born in Kobe, Japan, on January 28, 1958. He received the B.E. and M.E. degrees in electrical communication engineering from Osaka University, Osaka, Japan, in 1980 and 1982, respectively. He worked there on research in the areas of electromagnetic theory and optical waveguides.

He is presently with Kansai Electric Power Company, Osaka, Japan.

✤

Nobuaki Kumagai (M'59–SM'71–F'81) was born in Ryojun, Japan, on May 19, 1929. He received the B. Eng. and D. Eng. degrees from Osaka University, Osaka, Japan, in 1953 and 1959, respectively.

From 1956 to 1960 he was a Research Associate in the Department of Communication Engineering at Osaka University. From 1958 through 1960 he was a Visiting Senior Research Fellow at the Electronics Research Laboratory of the University of California, Berkeley, on leave of absence from Osaka University. From 1960 to 1970 he was an Associate Professor, and has been a Professor of Communication Engineering at Osaka University since 1971. He served as a Department Chairman in the periods of 1972–1973 and 1977–1978. From 1980 to 1982 he served as the Dean of Students of Osaka University.

His fields of interest are electromagnetic theory, microwaves, millimeter-waves, and acoustic-waves engineering, optical fibers and optical-fiber communication techniques, optical integrated circuits and devices, and lasers and their applications. He has published more than one hundred technical papers on these topics in established journals. He is the author or coauthor of several books including *Microwave Circuits* (OHM-sha, Tokyo, 1963) and *Introduction to Relativistic Electromagnetic Field theory* (Corona Publishing Co., Tokyo, 1971). From 1979 to 1981 he was President of the Microwave Theory and Techniques Society of the Institute of Electronics and Communication Engineers of Japan.

Dr. Kumagai is a member of the Institute of Electronics and Communication Engineers of Japan, the Institute of Electrical Engineers of Japan, and the Laser Society of Japan. He was elected a Fellow of the IEEE for contributions to the study of wave propagation in electromagnetics, optics, and acoustics.

Hollow Image Guide and Overlayed Image Guide Coupler

JING-FENG MIAO AND TATSUO ITOH, FELLOW, IEEE

Abstract—**A dielectric waveguide structure, hollow image guide, is described. This structure has several interesting characteristics useful for millimeter-wave applications. Dispersion characteristics and field distributions are theoretically and experimentally studied. The structure can also be considered as two parallel image guides coupled strongly by a dielectric overlay. Coupling characteristics between two image guide arms are studied numerically and experimentally.**

I. Introduction

RECENTLY, increasing attention has been paid to millimeter-wave circuits made of image-guide structures (Fig. 1(b)). It is often difficult to create a simple circuit for some signal processing functions with conventional image guides. Several attempts have been made to alleviate this difficulty [1], [2]. Both of these attempts modified the boundary conditions outside the dielectric rod of the waveguide. The new structure introduced in this paper modifies the interior of the dielectric rod. The structure may be called the hollow image guide (Fig. 1(a)). As shown in the figure, a portion of the dielectric material is removed from the rod (ϵ_2). The cross section of the hollow core (ϵ_1) has height h and width $2c$. The hollow core may be filled with another material if needed. The new waveguide can be used in conjunction with the techniques in [1] and [2]. However, the hollow image guide has a number of interesting features in its own right, making the design process more flexible. For instance, the hollow core may be used to control the field distribution outside the dielectric rod as well as the propagation constant without altering the exterior dimensions or the dielectric material. Also, by changing the core height gradually over some distance, we can create a smooth transition from the image guide to a solid-state device mounted in a hollow core.

The hollow image guide can also be thought of as two image guides (II in Fig. 1(a)) strongly coupled by way of a dielectric (I in Fig. 1(a)) or two image guides of height h coupled by an overlay of thickness of t. The degree of coupling can be adjusted by changing c, h, or b in Fig. 1(a).

In this paper, we study the propagation characteristics

Manuscript received April 8, 1982; revised June 2, 1982. This work was supported in part by the US Army Research Office, under Contract DAAG29-81-K-0053, and in part by the Joint Services Electronics Program, under Contract F49620-79-C-0101.

The authors are with the Department of Electrical Engineering, University of Texas, Austin, TX 78712.

0018-9480/82/1100-1826$00.75 ©1982 IEEE

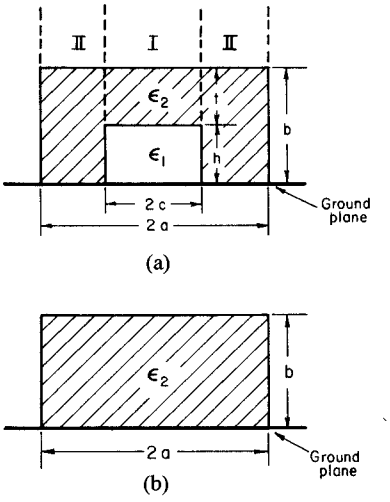

Fig. 1. Cross sections of dielectric guides. (a) Hollow image guides. (b) Image guide.

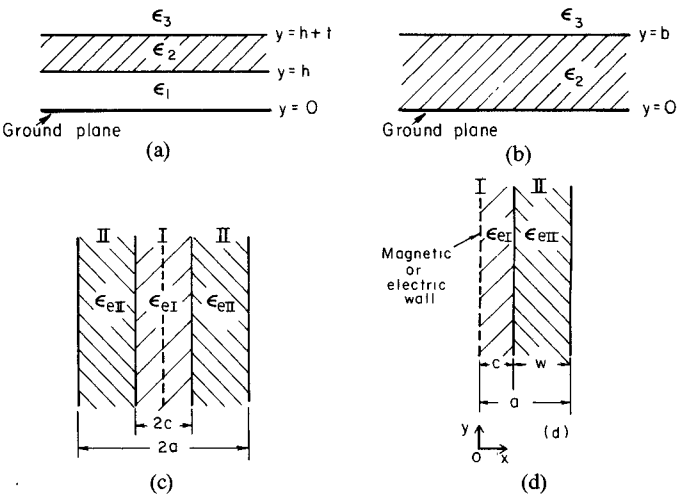

Fig. 2. Analytical process for the effective dielectric constant method. (a) Structure for ϵ_{eI}. (b) Structure for ϵ_{eII}. (c) Hypothetical structure for k_z. (d) One half of (c) due to symmetry.

and field distributions of the proposed structure and those properties are compared with those of the conventional image guide. Coupling characteristics of the hollow image guide when viewed as a coupled structure have been studied.

II. Dispersion Characteristics and Field Distributions

Since the hollow image guide is a modification of the image guide, the hybrid eigenmodes can be classified into E_{pq}^{y} and E_{pq}^{x} groups. Although more elaborate analysis methods are available, a simple effective dielectric constant (EDC) approach provides results accurate enough for most engineering applications, especially in dispersion characteristics [3]. Since the EDC procedure is well known [1], [3], only the key steps are summarized below. All the field components can be derived from

$$E_y = \frac{1}{\epsilon_r(y)}\left(k_z^2 - \frac{\partial^2}{\partial x^2}\right)\phi^e \tag{1}$$

$$H_y = \left(k_z^2 - \frac{\partial^2}{\partial x^2}\right)\phi^h \tag{2}$$

where $\epsilon_r(y)$ is a relative dielectric constant in the region of application and k_z is the propagation constant in the z direction. Since both E_{pq}^{y} and E_{pq}^{x} modes can be analyzed in a similar manner, we will only analyze the E_{pq}^{y} modes. In this case, ϕ^e has the dominant contribution and ϕ^h may be neglected.

We first obtain the effective dielectric constant ϵ_{eI} of Region I in Fig. 1(a). This quantity may be derived by solving the eigenvalue equation of the layered structure shown in Fig. 2(a). For such a structure, we write

$$\phi^e(y) = \cosh(\eta_1 y), \qquad 0 < y < h \tag{3}$$

$$\phi^e(y) = A_y \cos\left[k_y(y-h)\right] + B_y \sin\left[k_y(y-h)\right], \quad h < y < h + t = b \tag{4}$$

$$\phi^e(y) = C_y \exp\left[-\eta_3(y-b)\right], \qquad y > b \tag{5}$$

where k_y is the propagation constant in the y direction in the ϵ_2 layer and η_1 and η_3 are attenuation constants in the ϵ_1 and ϵ_3 regions. These constants are related via

$$\epsilon_3 k_0^2 < \epsilon_1 k_0^2 + \eta_1^2 = \epsilon_2 k_0^2 - k_y^2 = \epsilon_3 k_0^2 + \eta_3^2 = k_{zI}^2 < \epsilon_2 k_0^2 \tag{6}$$

where η_3 must be real and greater than zero. η_1 may be either real or imaginary, k_0 represents the free-space wavenumber, and k_{zI} is the propagation constant in the z direction in Fig. 2(a).

Matching the field components H_x and E_z at $y = h$ and $y = b$, we get the following eigenvalue equation:

$$-\frac{1}{\epsilon_2}k_y \sin(k_y t) + \left[\frac{1}{\epsilon_1}\eta_1 \tanh(\eta_1 h) + \frac{\eta_3}{\epsilon_3}\right]\cos(k_y t) + \frac{\epsilon_2 \eta_3}{\epsilon_1 \epsilon_3}\eta_1 \tanh(\eta_1 h)\frac{\sin(k_y t)}{k_y} = 0. \tag{7}$$

When this equation is solved for k_y, the effective dielectric constant ϵ_{eI} is given by

$$\epsilon_{eI} = \epsilon_2 - \left(\frac{k_y}{k_0}\right)^2. \tag{8}$$

In a similar manner, the effective dielectric constant ϵ_{eII} of Region II in Fig. 1(a) is

$$\epsilon_{eII} = \epsilon_2 - \left(\frac{k_y'}{k_0}\right)^2 \tag{9}$$

where k_y' is the solution of the eigenvalue equation

$$\frac{k_y'}{\epsilon_2}\sin(k_y' b) - \frac{\eta_3}{\epsilon_3}\cos(k_y' b) = 0 \tag{10}$$

for the layered structure in Fig. 2(b). Notice that both ϵ_{eI} and ϵ_{eII} are functions of frequency.

We are now ready to model the original structure in Fig. 1(a) with the hypothetical one shown in Fig. 2(c). This layered structure can be analyzed by using the eigenvalue equation. Because of the symmetry, we only need to con-

sider half the structure given in Fig. 2(d). All the field components can be derived from

$$\phi^e(x) = \frac{\cosh\{\xi_1 x\}}{\sinh\{\xi_1 x\}}, \qquad 0 < x < c \tag{11}$$

$$\phi^e(x) = A_x \cos\left[k_x(x-c)\right] + B_x \sin\left[k_x(x-c)\right], \quad c < x < a = c + w \tag{12}$$

$$\phi^e(x) = C_x \exp\left[-\xi_3(x-a)\right], \qquad x > a. \tag{13}$$

By matching appropriate field components at the dielectric interfaces, we obtain the following eigenvalue equation:

$$\left[k_x \sin(k_x w) - \xi_3 \cos(k_x w)\right] - \left[\cos(k_x w) + \xi_3 \frac{\sin(k_x w)}{k_x}\right] \xi_1 \begin{Bmatrix} \tanh(\xi_1 c) \\ \coth(\xi_1 c) \end{Bmatrix} = 0 \tag{14}$$

where the tanh and coth correspond to the magnetic and electric walls in Fig. 2(d). The propagation constant k_z of the original structure is assumed to be given by the solution k_x of (14) as

$$k_z^2 = \epsilon_{e\Pi} k_0^2 - k_x^2. \tag{15}$$

From the solution k_y of (7), the field amplitude coefficients A_y, B_y, and C_y in (4) and (5) can be calculated. Similarly, A_x, B_x, and C_x in (12) and (13) can be derived from the solution k_x of (14). Hence, the cross-sectional field distributions can readily be obtained. Notice, however, that the field distributions so obtained are only approximate. They are generally correct qualitatively, but not quantitatively. This is in contrast to accurate solutions attainable for k_z. The reason for this deficiency lies in the fact that the effective dielectric constant method is basically a one-mode approximation of the more sophisticated transverse resonance technique involving infinitely many modes in constituent regions and the junction effect therebetween [3]. The one-mode approximation neglects all of these detailed field behaviors. However, it is widely known that accuracy of the propagation constant k_z is surprisingly good for most cases of engineering interest.

Finally, we note that all the analyses and numerical procedures are applicable to the case of image guide by simply letting either c or h to zero.

III. Numerical and Experimental Results

Fig. 3 shows dispersion characteristics of the dominant E_{11}^y mode and the first odd mode E_{21}^y of hollow image guides with identical exterior dimensions but with two different hollow core sizes. For comparison, we also included the dispersion characteristics of an image guide with exterior dimensions identical to those of the hollow image guides. It is evident that the propagation constant can be altered by changing the dimensions of the hollow core.

The E_y field of the dominant E_{11}^y mode was computed as a function of the sideward (x) coordinate for both the hollow guides and the image guide with identical exterior dimensions (Fig. 4). It is clear that the peak of the field is shifted toward the sidewalls in the hollow image guide. It can also be seen that outside the guides the field distribu-

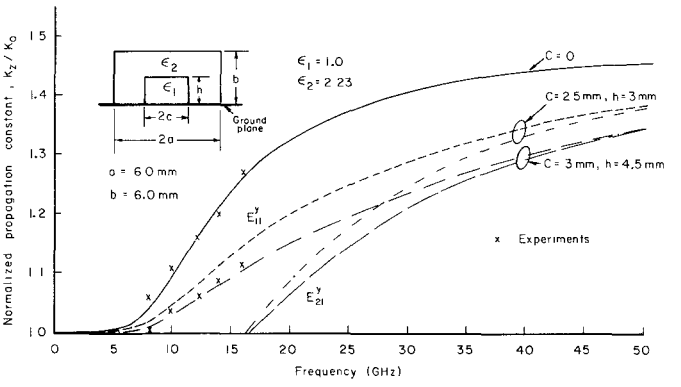

Fig. 3. Dispersion characteristics.

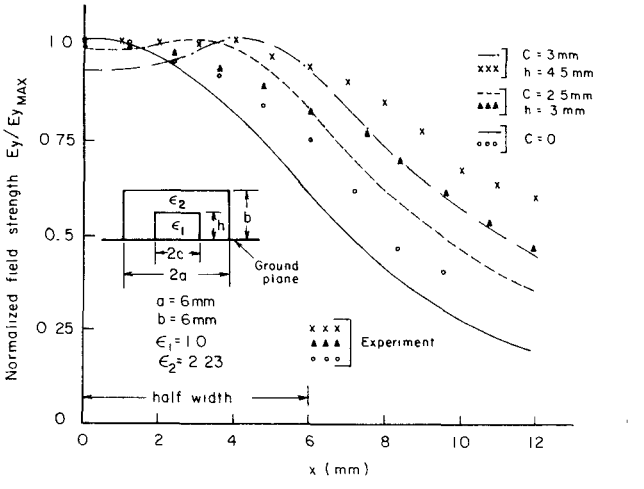

Fig. 4. Field distributions in the transverse direction. The measurement was done 3 mm above the rod top surface (9 mm above the ground plane) at 14 GHz.

tion of hollow image guide is higher than that of image guides. For instance, at $x = 9$ mm (3 mm away from the sidewall), the E_y field of the hollow image guide ($c = 2.5$ mm, $h = 3.0$ mm) is 19 percent higher. It should be noted that the field plots are normalized to the peak values of each curve. Therefore, the absolute values of peaks are not necessarily the same. However, in most cases such difference was quite small.

Since the propagation constant can be adjusted by changing the size of the hollow core, we can in turn design a hollow image guide with larger exterior dimensions than the image guide but with identical propagation constant. Fig. 5 shows comparison of the field distributions in such structures. The field outside the hollow guide is still stronger than that of the image guide, but the difference is smaller than the situation in Fig. 4. In fact, at 9 mm from the center of both guides, the difference is only 12 percent.

The propagation constants and the field distributions have been measured by means of a movable electric field probe [4]. Due to the equipment limitation, the measurement was done in the frequency range between 8 and 16 GHz. For the dispersion characteristics, a metal plate was placed on the dielectric rod so that a partially reflected wave creates a standing wave which is in turn detected by the probe. From the standing wave patterns we can get propagation constants. Some results are ploted on Fig. 3

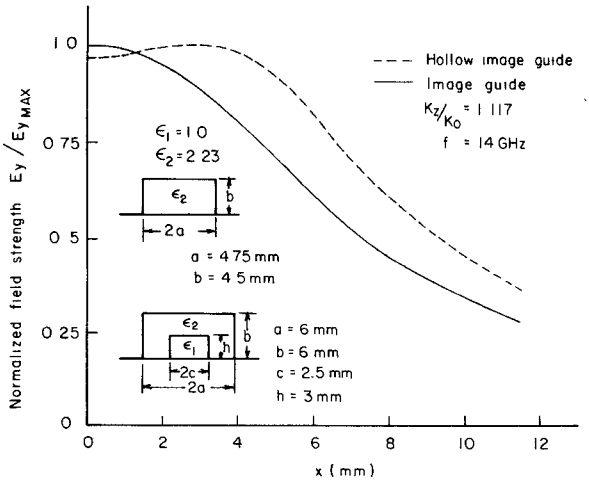

Fig. 5. Field distributions for the image guide and the hollow image guide with identical propagation constants.

and agreement with theoretical data is seen to be quite good.

The field distributions can also be measured by moving the probe in the transverse direction. The results plotted in Fig. 4 do not provide as good agreement with the theory as those for propagation constants. This is because, as mentioned earlier, the field calculated by the effective dielectric constant method does not result in as accurate a solution as the propagation constant. However, qualitative agreement between theory and experiment is satisfactory.

IV. Coupling Characteristics

The hollow image guide can be viewed as two image guides coupled by a dielectric bridge; therefore, we know that above a certain frequency there exists symmetric and antisymmetric modes as shown in Fig. 3. By using the characteristics of the even mode E_{11}^y and first odd mode E_{21}^y, one can make directional couplers which are very important both in passive and active components of millimeter-wave integrated circuits.

It is well known that leakage due to discontinuities and irregularities exist in dielectric waveguides. In addition, a field component which takes the form of lateral leakage (in the form of a surface wave) could exist in Region I even if the structure is perfect [3]. If the latter is the case, the coupling mechanism would be more complicated and is expected to be stronger. However, in the present analysis, such a lateral leakage field is not taken into consideration.

As is known, it is the interaction of even and odd modes traveling with different phase velocities along the z direction that represents the effect of coupling. We define $K = (k_{ze} - k_{z0})/(k_{ze} + k_{z0})$ as the degree of coupling, where k_{ze} and k_{z0} are the propagation constants of the even (E_{11}^y) and the odd (E_{21}^y) modes. The degree of the coupling of the hollow image guide with certain exterior dimensions are computed for different values of h and c and are shown in Fig. 6(a) and (b). From Fig. 6 we can see that the larger the cross section of the hollow core, the smaller is the degree of coupling. The point for $h = 6$ mm ($= b$) in Fig. 6(b) corresponds to the situation of coupled image guides. From Fig. 6 we can also see that, in order to

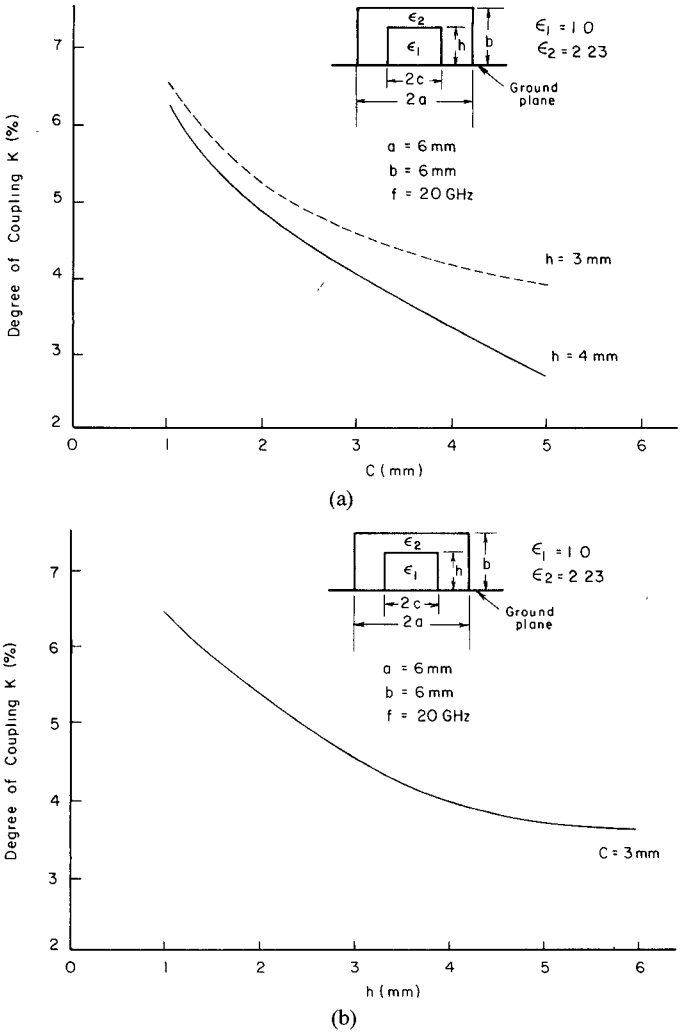

Fig. 6. Degree of coupling $K = k_{ze} - k_{z0}/k_{ze} + k_{z0}$. (a) K (percent) versus core width. (b) K (percent) versus core height.

change the degree of coupling, one can change c, h, or b. This interesting feature can be used to make the design process of directional couplers more flexible than that of the coupled dielectric image guides [5]. In fact, a directional coupler fabricated by Paul and Chang [6] has a grounded dielectric bridge. It is similar to the directional coupler reported in this paper, except that their structure is realized by flipping over the present directional coupler. The motivation of such a structure is to improve mechanical stability.

Because of the coupling characteristic of hollow image guides, a wave incident from Port 1 couples part of its energy to Port 3 as shown in Fig. 7. If the hollow image guide is lossless and is matched in every port, then in order to transfer the total power of the incident wave from Port 1 to Port 3, the length L of the hollow image guide must be

$$L = \frac{\pi}{k_{ze} - k_{z0}}. \tag{16}$$

For a 3-dB directional coupler, the length must be

$$L_{3\text{dB}} = \frac{\pi}{2(k_{ze} - k_{z0})} = L/2. \tag{17}$$

The scattering coefficients for the hollow image guide

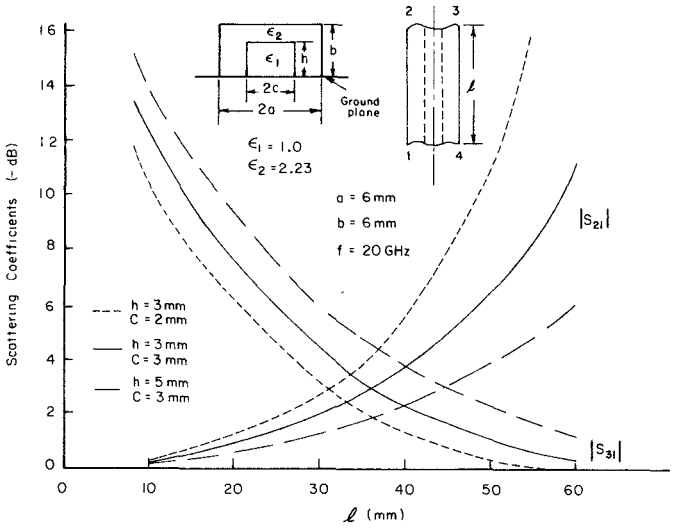

Fig. 7. Scattering coefficients versus length for different values of core sizes.

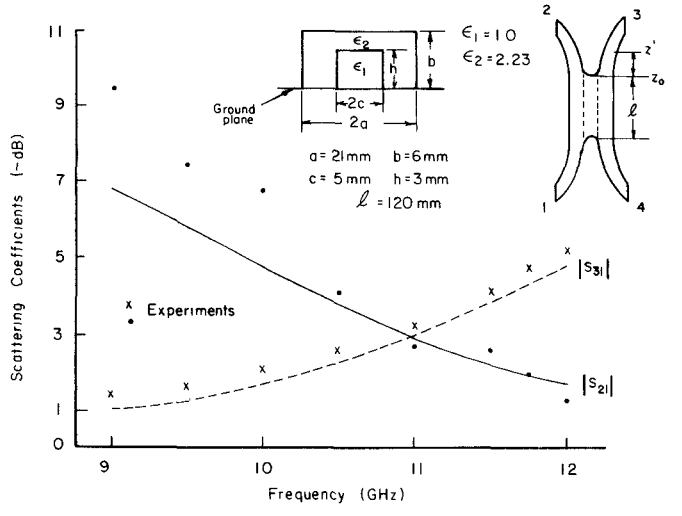

Fig. 8. Frequency characteristics of a 3-dB directional coupler ($l = 120$ mm, $l_e = 192$ mm).

can be expressed as follows:

$$|S_{21}| = \left|\cos\frac{k_{ze} - k_{z0}}{2} l\right| \tag{18}$$

$$|S_{31}| = \left|\sin\frac{k_{ze} - k_{z0}}{2} l\right|. \tag{19}$$

The scattering coefficients of the hollow image guides with different lengths and cross sections are computed and shown in Fig. 7. By changing l, h, or c, different scattering coefficients can be obtained. The value of l required for 3-dB directional coupler ($= L_{3dB}$) can be read from the intersection of $|S_{21}|$ and $|S_{31}|$ curves.

We fabricated a 3-dB directional coupler out of a hollow image guide. The measured and computed frequency characteristics are shown in Fig. 8. In theoretical calculations, the effective length l_e, is obtained by using the following equations [7]:

$$l_e = l + \frac{\Delta\phi}{\pi} L \tag{20}$$

and

$$\Delta\phi = \int_{z_0}^{z'} [k_{ze}(z) - k_{z0}(z)]\, dz \tag{21}$$

where z_0 corresponds to the junction between the coupled guide and the connecting arms, which are conventional image guides, and z' is chosen to be a value for which the coupling between the arms is negligible.

The measured data shown in Fig. 8 have been corrected for the dielectric and radiation losses at the bends and junctions of the waveguide (using substitution method). At lower frequencies, the radiation from the waveguide is very strong because the wave is not tightly coupled to the dielectric rod. Therefore, the measured values of power transfer to Ports 2 and 3 are smaller than the theoretical values. This discrepancy becomes smaller at higher frequencies where the wave is more tightly confined in the waveguide and the radiation loss at junctions and bends becomes smaller. In general, however, qualitative agreement between theory and experiment is satisfactory. We have not plotted S_{41} in Fig. 8 since it was negligibly small (less than -30 dB).

V. Conclusions

In this paper, a novel waveguide structure—hollow image guide—has been studied both theoretically and experimentally, and comparisons have been made between the hollow image guide and image guide in propagation constant, and field distribution, coupling characteristic. The comparisons show that the hollow image guide is a useful dielectric waveguide for millimeter-wave integrated circuits although its field distribution outside of the guide is a little higher than that of the image guide. The structure can be used to make the design process more flexible. In addition, it can be used in conjunction with other dielectric waveguides in millimeter-wave integrated circuits and in creating a smooth transition from the image guide to a solid-state device.

The hollow image guide can be used as a directional coupler connecting four image guide ports. The design process is again more flexible than that for the coupler made of image guides placed in parallel because the thickness of the overlay ($b-h$ in Fig. 1) can be adjusted for a desired degree of coupling.

References

[1] T. Itoh and B. Adelseck, "Trapped image guide for millimeter-wave circuits," *IEEE Trans. Microwave Theory Tech.*, vol. MTT-28, pp. 1433–1436, Dec. 1980.

[2] T. Yoneyama and S. Nishida, "Nonradiative dielectric waveguide for millimeter-wave integrated circuits," *IEEE Trans. Microwave Theory Tech.*, vol. MTT-29, pp. 118–1192, Nov. 1981.

[3] S. T. Peng and A. A. Oliner, "Guidance and leakage properties of a class of open dielectric waveguides: Part I–Mathematical formulations," *IEEE Trans. Microwave Theory Tech.*, vol. MTT-29, pp. 843–854, Sept. 1981.

[4] K. Solbach, "Electric probe measurements on dielectric image lines in the frequency range of 20–90 GHz," *IEEE Trans. Microwave Theory Tech.*, vol. MTT-26, pp. 755–758, Oct. 1978.

[5] K. Solbach, "The calculation and the measurement of the coupling properties of dielectric image lines of rectangular cross sections," *IEEE Trans. Microwave Theory Tech.*, vol. MTT-27, pp. 54–58, Jan. 1979.

[6] J. A. Paul and Y.-W. Chang, "Millimeter-wave image-guide integrated passive devices," *IEEE Trans. Microwave Theory Tech.*, vol. MTT-26, pp. 751–754, Oct. 1978.
[7] R. Rudokas and T. Itoh, "Passive millimeter-wave IC components made of inverted strip dielectric waveguides," *IEEE Trans. Microwave Theory Tech.*, vol. MTT-24, pp. 978–981, Oct. 1976.

Jing-Feng Miao was born in Jiangsu Province, China, on January 10, 1937. He graduated from Nanjing Institute of Technology, Nanjing, China, in 1962.

Currently, he is a faculty member of the Radio Engineering Department, Nanjing Institute of Technology, doing teaching and research work in the field of microwave devices and circuits. From August 1981 to August 1982 he was a Visiting Scholar at the University of Texas at Austin, in the Department of Electrical Engineering. His research interest is mainly in microwave solid-state devices and circuits, and millimeter-wave integrated circuits.

Tatsuo Itoh (S'69–M'69–SM'74–F'82) received the Ph.D. degree in electrical engineering from the University of Illinois, Urbana in 1969.

From September 1966 to April 1976 he was with the Electrical Engineering Department University of Illinois. From April 1976 to August 1977 he was a Senior Research Engineer in the Radio Physics Laboratory, SRI International, Menlo Park, CA. From August 1977 to June 1978 he was an Associate Professor at the University of Kentucky, Lexington, In July 1978 he joined the faculty at the University of Texas at Austin, where he is now a Professor of Electrical Engineering and Director of Microwave Laboratory. During the summer 1979 he was a Guest Researcher at AEG-Telefunken, Ulm, West Germany.

Dr. Itoh is a member of the Institute of Electronics and Communication engineers of Japan, Sigma Si, and Commission B of USNC/URSI. He serves on the Administrative Committee of IEEE Microwave Theory and Techniques Society. He is a Professional Engineer registered in the State of Texas.

Biological Effects and Medical Applications of RF Electromagnetic Fields

OM P. GANDHI, FELLOW, IEEE

(*Invited Paper*)

Abstract—**The paper summarizes replicable biobehavioral effects including ocular and auditory effects and the low-level efflux of calcium ions from chick and cat cortex tissues exposed to sinusoidally modulated fields. Highlights of studies of long-term and ultra-long-term low-level exposures on rat behavior and blood and urine biochemistry are also given. The new ANSI C95 recommended safety standard and its rationale are presented, as are some of the present and potential medical applications including hyperthermia for cancer therapy. The paper concludes with identified gaps in knowledge where more research is needed.**

I. Introduction

THERE IS a great deal of concern on the part of the public about the purported biohazards of RF electromagnetic radiation, and also an anticipation among the researchers in this area of beneficial medical applications such as for electromagnetic hyperthermia as an adjunct for cancer therapy, electromagnetic heating for blood and organ thawing and for hypothermia, and also the possibility of the use of this radiation for diagnostic imaging applications. Among the (popular press) reported effects of microwave radiation are: cataract formation, fatigue, sleeplessness, sexual dysfunction, carcinogenic properties, etc. Name a malady and it has been ascribed to microwave radiation. Unfortunately, the adverse publicity given the alleged biohazards of nonionizing radiation has conditioned the public to be suspicious of any and all of the applications of this energy. This has resulted in obstructive and costly litigation and unnecessary delays in new installations in the public domain even of the types that were set up without questions in the past. An example here is the microwave repeater stations, hundreds of which were set

Manuscript received July 14, 1982. This paper is based in part on a presentation by the author at the joint plenary session of the URSI and IEEE-MTT and AP Symposia, (Los Angeles, CA) on June 17, 1981.

The author is with the Department of Electrical Engineering, University of Utah, Salt Lake City, UT 84112.

0018-9480/82/1100-1831$00.75 ©1982 IEEE